

# Growth of Low-Density Vertical Quantum Dot Molecules with Control in Energy Emission

P. Alonso-González · L. González · J. Martín-Sánchez ·  
Y. González · D. Fuster · D. L. Sales · D. Hernández-Maldonado ·  
M. Herrera · S. I. Molina

Received: 23 June 2010 / Accepted: 18 August 2010 / Published online: 5 September 2010  
© The Author(s) 2010. This article is published with open access at Springerlink.com

**Abstract** In this work, we present results on the formation of vertical molecule structures formed by two vertically aligned InAs quantum dots (QD) in which a deliberate control of energy emission is achieved. The emission energy of the first layer of QD forming the molecule can be tuned by the deposition of controlled amounts of InAs at a nanohole template formed by GaAs droplet epitaxy. The QD of the second layer are formed directly on top of the buried ones by a strain-driven process. In this way, either symmetric or asymmetric vertically coupled structures can be obtained. As a characteristic when using a droplet epitaxy patterning process, the density of quantum dot molecules finally obtained is low enough ( $2 \times 10^8 \text{ cm}^{-2}$ ) to permit their integration as active elements in advanced photonic devices where spectroscopic studies at the single nanostructure level are required.

**Keywords** Molecular beam epitaxy · Droplet epitaxy · Quantum dots

The simplest interacting quantum dot (QD) system is a QD molecule (QDM) composed of two closely spaced QD [1–3]. QDM are receiving much attention both as playground for studying coupling and energy transfer processes between “artificial atoms” and as new systems, which substantially extend the range of possible applications of QD [4]. In such systems, the coupling involves tunneling of electrons and holes between two adjacent dots separated by a thin intermediate barrier layer. In particular, it has been observed [5] that for a 4-nm-thick intermediate tunneling layer, the coupling strength is optimized for the spectroscopic observation of large electron anti-crossing energy splitting [5]. It is, however, technologically challenging to obtain resonant quantum–mechanical coupling due to size, composition, and strain inhomogeneities inherent in self-assembled QD. In this sense, great efforts have been dedicated to the formation of vertical coupled QD by self-assembling processes [6]. The most used fabrication process leading to vertically aligned QD is based on the formation of one layer of self-assembled QD, followed by a thin spacer layer. Then, upon further InAs deposition, a second layer of QD is formed, on top of the buried QD, by strain-driven processes. By this growth procedure, tuning of the emission energy of one of the QD at the same time that is maintained unaltered the emission properties of the other, although not impossible, is difficult to achieve due to the lack of control in size for self-assembled QD. The tuning effect of the emission energy of one of the QD forming the molecule respect to the other would permit to build symmetric vertical QDM, in which the energy emission of both QD forming the molecule matches, and asymmetric vertical QDM, in which the energy emission of one QD is blue-shifted or red-shifted respect to the other [5–7]. Apart from this lack of control in size of the QD forming the QDM by a self-assembling process, there is an

P. Alonso-González (✉) · L. González · J. Martín-Sánchez ·  
Y. González  
Instituto de Microelectrónica de Madrid (IMM-CNM, CSIC),  
Isaac Newton, 8 Tres Cantos, 28760 Madrid, Spain  
e-mail: palonso@nanogune.eu

D. Fuster  
UMDO (Unidad Asociada al CSIC-IMM), Instituto de Ciencia  
de Materiales, Universidad de Valencia, P.O. Box 22085,  
4607 Valencia, Spain

D. L. Sales · D. Hernández-Maldonado · M. Herrera ·  
S. I. Molina  
Departamento de Ciencia de los Materiales e I.M. y Q.I,  
Universidad de Cádiz, Puerto Real, 11510 Cádiz, Spain

intrinsic inter-dependent nature between the QD size and density that makes difficult the design of QD of a desired size and with a low enough density for its spectroscopic study at the single nanostructure level [8–10].

In this sense, here, we present a process that optimizes the growth of coupled structures in vertical arrangement by the use of a low-density nanoholes template fabricated by droplet epitaxy [11]. In particular, after the deposition of the designed amount of InAs on the template that permits the formation of a first layer of size controlled nanostructures [12], a thin GaAs layer is grown to create a carrier tunneling barrier that separates a second layer of InAs nanostructures formed, via a strain-driven process, on top of the first ones.

Thus, the growth procedure starts with the filling of previously formed nanoholes with InAs material. As detailed in [9], the nanoholes appear with a density of  $2 \times 10^8 \text{ cm}^{-2}$ , and they are  $4.4 \pm 0.8 \text{ nm}$  in depth with a mean diameter of  $43 \pm 3 \text{ nm}$  at their half maximum. On this pattern, three samples with different amount of InAs, 1.2, 1.4 and 1.5 monolayers (ML), have been grown at a substrate temperature of  $500^\circ\text{C}$ , growth rate  $r_g(\text{InAs}) = 0.01 \text{ ML/s}$ , and  $\text{As}_4$  beam equivalent pressure  $\text{BEPAs}_4 = 5\text{--}10^{-7} \text{ Torr}$ .

Once formed the first layer of QD ( $\text{QD}_1$  hereinafter), a GaAs intermediate barrier with a thickness of 4 nm is subsequently grown to guarantee a large tunneling effect [5]. The growth of this layer is performed by atomic layer molecular beam epitaxy (ALMBE) growth technique [13] at a substrate temperature  $T_s = 450^\circ\text{C}$ , growth rate  $r_{g\text{GaAs}} = 0.5 \text{ ML/s}$ , and beam equivalent pressure  $\text{BEPAs}_4 = 2 \times 10^{-6} \text{ Torr}$ . At this moment, for completing the molecule structure, a second layer of QD ( $\text{QD}_2$  hereinafter), located above the  $\text{QD}_1$ , is grown by the deposition of 0.9 ML of InAs at the same conditions used for the underlying nanostructures.

With the aim of studying the optical emission of the resulting QD molecule structures, a 155-nm-thick GaAs layer is finally grown. A schematic diagram of these samples is shown in Fig. 1.

Transmission electron microscopy images have been obtained to know the structural configuration of the resulting molecules. Figure 2a and b shows 002 dark field (cross-sections) transmission electron microscopy (TEM) images for the samples with 1.4 and 1.2 ML of InAs deposited into the nanoholes forming the  $\text{QD}_1$  layer. Contrast in this image is due to changes in composition, dark areas indicating the presence of In in In(Ga)As layers. It can be observed the formation of the double structure that consists of two InAs QD separated by the 4-nm-thick GaAs barrier layer. Their respective wetting layers (WLs) are also clearly observed. It is noticeable that as a difference to the strain-driven formation of  $\text{QD}_2$ , or in general, in

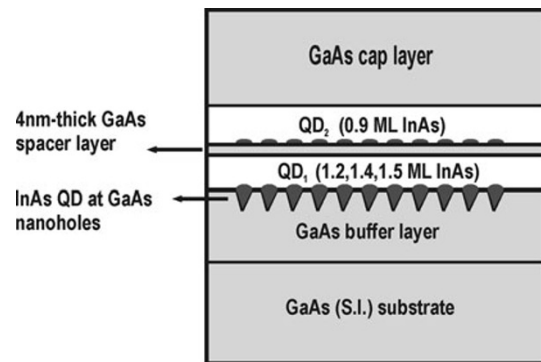


**Fig. 1** Schematic diagram of the samples grown for obtaining vertical QD molecule structures. The first layer of nanostructures ( $\text{QD}_1$ ), is formed after depositing 1.2, 1.4, and 1.5 ML of InAs into GaAs nanoholes previously formed by droplet epitaxy. After the growth of 4-nm-thick GaAs barrier layer, a second layer of nanostructures ( $\text{QD}_2$ ) is formed on top of  $\text{QD}_1$  by a stress induced growth process when 0.9 ML of InAs is deposited

a self-assembling process,  $\text{QD}_1$  forms at a lower level than the WL, clearly indicating a formation mechanism that involves preferential nucleation of InAs material into previously fabricated GaAs nanoholes by droplet epitaxy [12].

In the case of depositing 1.4 ML of InAs (Fig. 2a),  $\text{QD}_1$  clearly presents a larger size than  $\text{QD}_2$  nucleated on top of it. On the other hand, when 1.2 ML of InAs are deposited (Fig. 2b),  $\text{QD}_1$  is more similar in size to  $\text{QD}_2$ . According to these results, the aimed tuning effect on the size of  $\text{QD}_1$  by the use of nanoholes has been successfully obtained. On the

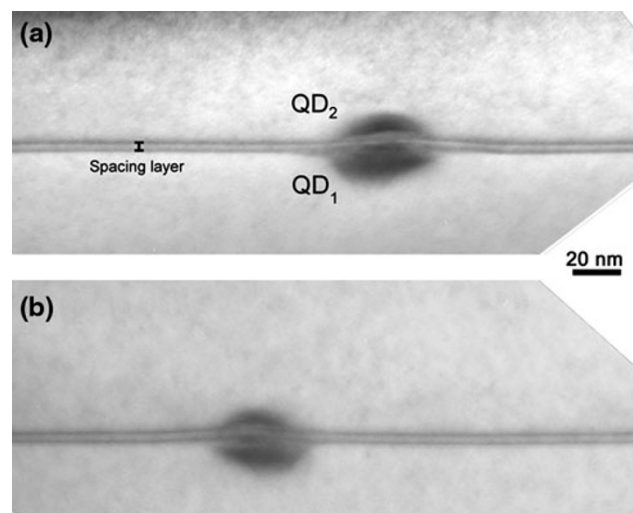


**Fig. 2** a 002 dark field (cross-section) transmission electron microscopy (TEM) images of two vertically aligned QD formed after depositing 1.4 ML of InAs into a GaAs nanohole ( $\text{QD}_1$ ), the growth of 4-nm-thick GaAs barrier acting as tunneling layer and a final deposition of 0.9 ML of InAs ( $\text{QD}_2$ ). We observe that in this case,  $\text{QD}_1$  is larger in size than  $\text{QD}_2$ . b TEM image of the formed structure when 1.2 ML of InAs is deposited to form the  $\text{QD}_1$  nanostructures. In this case, it can be observed that  $\text{QD}_1$  is now quite similar in size to  $\text{QD}_2$

other hand, despite this engineered change in size of QD<sub>1</sub>, the nucleation of QD<sub>2</sub> takes place on top of the buried QD<sub>1</sub> with same density of QD<sub>1</sub> layer and similar dimensions in all cases. These results show that the size of the strain driven formed QD<sub>2</sub> is controlled by the amount of InAs deposited. Moreover, the strain gradient at the surface is large enough to promote preferential nucleation of InAs just on top of the buried QD<sub>1</sub>, even for InAs deposited thickness of 0.9 ML, which is much lower than the critical thickness for QD formation in absence of local strain fields [14].

Concerning the optical properties of these paired nanostructures, Fig. 3 shows the PL signal for the three different cases. In particular, the black, red, and blue lines in the figure correspond to QD pair structures obtained by depositing 1.2, 1.4, and 1.5 ML of InAs for the formation of QD<sub>1</sub> layer, respectively. The presence of two main peaks can be observed in all the cases. The evolution of these two PL peaks with increasing excitation power (not shown) reveals that they correspond to two different QD families, as they do not show any relative saturation effects corresponding to one QD family with ground and excited states. Combining these optical emission results with those obtained by TEM structural analysis, it can be established a direct correspondence of the different emission energies to the recombination of carriers at the upper and lower QD layers of the molecule structure. Figure 4a shows as filled areas the three different PL emissions that would correspond to the QD<sub>1</sub> family for the three different QD paired structures. As expected from previous results [12], the effect of the different amount of InAs deposited in the first

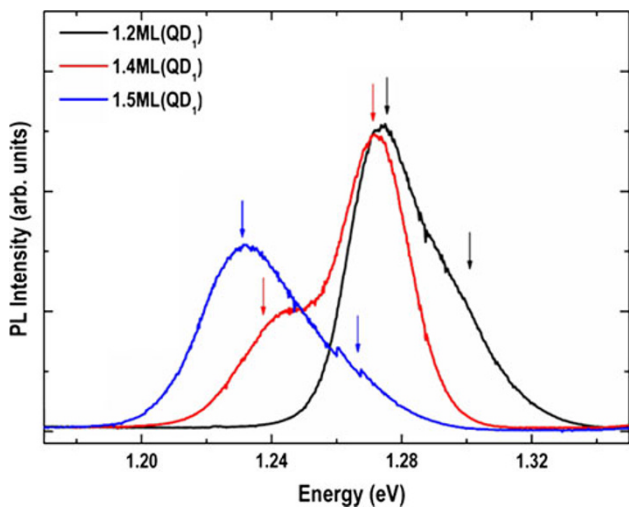


**Fig. 3** Photoluminescence spectra of the three different vertical QD pairs studied in this work. Black, red, and blue lines correspond to samples in which the QD<sub>1</sub> nanostructure layer is formed by depositing 1.2, 1.4, and 1.5 ML of InAs, respectively. The arrows in the figure point out the two families of QD formed in each sample

layer of nanostructures permits the emission energy of the QD<sub>1</sub> to be tuned in a wide range.

Table 1 lists the different values of the emission energies ascribed to QD<sub>1</sub> and QD<sub>2</sub> in the molecule structures. The arrow highlights the increase in PL emission peak energy of QD<sub>1</sub> with InAs deposited.

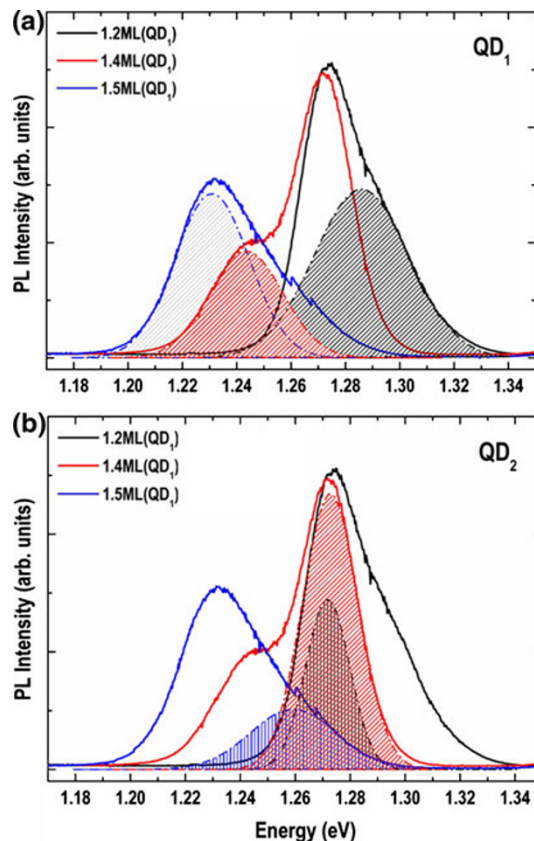


**Fig. 4** Photoluminescence emission (filled areas) ascribed to QD<sub>1</sub> (a) and QD<sub>2</sub> (b) nanostructures for 1.2, 1.4, and 1.5 ML of InAs deposited to form the QD<sub>1</sub> layer. It can be clearly shown in (a) a tuning effect on the emission energy of QD<sub>1</sub>. On the other hand, (b) shows that the emission corresponding to QD<sub>2</sub> layer remains almost unaltered despite the difference in size in QD<sub>1</sub>

**Table 1** PL emission peak energies ascribed to QD<sub>1</sub> and QD<sub>2</sub> layers

InAs (ML) QD <sub>1</sub>	InAs (ML) QD <sub>2</sub>	Peak energy (eV)	
		QD <sub>1</sub>	QD <sub>2</sub>
1.2	0.9	1.286	1.272
1.4	0.9	1.243	1.272
1.5	0.9	1.230	1.260

The QD<sub>1</sub> layer emission energy decreases as a function of the amount of InAs deposited. An arrow in the table accounts for this tuning effect. On the other hand, the emission energy of the second layer of nanostructures (QD<sub>2</sub>) remains almost constant for the three different structures

In a similar way, Fig. 4b shows the emission of the remaining three PL peaks that would correspond to the QD<sub>2</sub> family in the QD paired structures. It can be observed that the emission energies are similar in all the cases showing that the size of the nanostructures formed in the QD<sub>2</sub> layer remains almost invariable despite the different amount of InAs deposited underneath (see PL energy values in Table 1).

More experimental work is needed to demonstrate if these paired QD structures show electronic coupling as corresponding to QD molecules.

Altogether, these results show that by varying the amount of InAs material deposited at a nanoholes template formed by droplet epitaxy, the emission of a first layer of QD can be tuned to obtain either a symmetric or an asymmetric vertically coupled QDM. As a characteristic when using a droplet epitaxy patterning process, the density of QD molecules obtained is low enough ( $2 \times 10^8 \text{ cm}^{-2}$ ) to permit their integration as active elements in advanced photonic devices where spectroscopic studies at the single nanostructure level are mandatory.

**Acknowledgments** The authors wish to acknowledge to Spanish MICINN through projects Consolider-Ingenio 2010 QOIT (CSD2006-0019) and IMAGINE (CSD2009-00013), NANINPHO-QD (TEC2008-06756-C03-01/03 and 02), the Junta de Andalucía (PAI research group TEP-120 and project P08-TEP-03516) and CAM 2010 Q&CLight (S2009ESP-1503).

**Open Access** This article is distributed under the terms of the Creative Commons Attribution Noncommercial License which permits any noncommercial use, distribution, and reproduction in any medium, provided the original author(s) and source are credited.

## References

1. S. Kiravittaya, A. Rastelli, O.G. Schmidt, *Rep. Prog. Phys.* **72**, 046502 (2009)
2. L. Wang, A. Rastelli, S. Kiravittaya, M. Benyoucef, O.G. Schmidt, *Adv. Mater.* **21**, 1 (2009)
3. P. Alonso-González, J. Martín-Sánchez, Y. González, B. Alén, D. Fuster, L. González, *Cryst. Growth Des.* **9**, 5–2525 (2009)
4. P. Borri, W. Langbein, U. Woggon, M. Schwab, M. Bayer, S. Fafard, Z. Wasilewski, P. Hawrylak, *Phys. Rev. Lett.* **91**, 267401 (2003)
5. H.J. Krenner, M. Sabathil, E.C. Clark, A. Kress, D. Schuh, M. Bichler, G. Abstreiter, J.J. Finley, *Phys. Rev. Lett.* **94**, 057402 (2005)
6. E.A. Stinaff, M. Scheibner, A.S. Bracker, I.V. Ponomarev, V.L. Korenev, M.E. Ware, M.F. Doty, T.L. Reinecke, D. Gammon, *Science* **311**, 636 (2006)
7. G.G. Tarasov, Z.Y. Zhuchenko, M.P. Lisitsa, Y.I. Mazur, Zh.M. Wang, G.J. Salamo, T. Warming, D. Bimberg, H. Kissel, *Semiconductors* **40**, 79 (2006)
8. Z.R. Wasilewski, S. Fafard, J.P. McCaffrey, *J. Cryst. Growth* **201**, 1131 (1999)
9. P. Alonso-González, B. Alén, D. Fuster, Y. González, L. González, J. Martínez-Pastor, *Appl. Phys. Lett.* **91**, 163104 (2007)
10. P. Alonso-González, L. González, D. Fuster, J. Martín-Sánchez, Y. González, *Nanoscale Res. Lett.* **4**, 873 (2009)
11. Zh.M. Wang, B.L. Liang, K.A. Sablon, G.J. Salamo, *Appl. Phys. Lett.* **90**, 113120 (2007)
12. P. Alonso-González, D. Fuster, L. González, J. Martín-Sánchez, Y. González, *Appl. Phys. Lett.* **93**, 183106 (2008)
13. F. Briones, L. González, A. Ruiz, *Appl. Phys. A* **49**, 729 (1989)
14. D. Fuster, M.U. González, L. González, Y. González, T. Ben, A. Ponce, S.I. Molina, *Appl. Phys. Lett.* **84**, 4723 (2004)